[Now published in full after the initial publication as an Epub ahead of print on July 11, 2021 at www.fluorideresearch.online/epub/files/131.pdf]

FLUORIDE REMOVAL FROM AQUEOUS SOLUTION BY ALMOND SHELL ACTIVATED CARBON

Hamideh Akbari,[a] Davood Balarak,[b] Maseoud Yousefi,[a] Parisa Rigi,[c] Amir Hossein Mahvi[d,e,*]

Tehran, Shiraz, and Zahedan, Iran

ABSTRACT: Fluoride (F^-), the ion of the element fluorine, is one of the mineral elements present in nature that enters drinking water through underground aquifers and when present in high concentration it can lead to risks such as skeletal, dental, and non-skeletal fluorosis with morbidity such as decreased IQ and negative effects on brain development, tooth discolouration, and bone pain. The aim of the study, was to study the ability of activated carbon developed from almond shell (ACAS), to remove fluoride from an aqueous solution. We examined the effects on fluoride removal efficiency of contact time, initial F^- concentration, pH, and ACAS mass. The equilibrium data were also examined with models including the Langmuir, Freundlich, and Temkin isotherms. The removal characteristics were validated through the use of different kinetic models for the estimation of the solute interaction and the nature of the biosorption. A contact time of 60 min, an adsorbent dosage of 0.6 g/L, and a pH of 3 were considered to be the optimal operational conditions. The biosorption of F^- onto ACAS and the equilibrium data follow from the Langmuir adsorption isotherm with a maximum adsorption of 84.3 mg/g and a regression coefficient of R^2=0.999. The kinetic studies showed that the system fitted the pseudo-second order kinetic model. Thus, this work gives new insights on the interaction of ACAS with F^- in a reconstituted aqueous solution.

Keywords: Activated carbon; Almond shell; Fluoride; Kinetics; Isotherms.

INTRODUCTION:

The sources of fluorine in water and soil are mostly geogenic and include several rock forming minerals.[1-4] The load of the fluoride ion (F^-) in water is also increased by various industries, such as those producing pesticides, ceramics, refrigerants, and aerosol propellants, Teflon cookware, and glassware.[5,6] Fluoride is considered to be able to prevent dental caries by decreasing the rate of demineralization of dental enamel and reversing the progression of existing decay by promoting the rate of remineralization.[7-9]

Various values have been given for the permissible limit for the fluoride concentration in potable water with the World Health Organization (WHO) recommending a desirable upper limit of fluoride in drinking water of 1.5 mg/L.[10-12] However, countries can set their own country standards and lower standards have been set of 0.6 mg/L in Senegal, West Africa, and 1 mg/L in India with a rider to the Indian limit of "the lesser the fluoride the better, as fluoride is injurious to health." In 2015, in the United States of America, a recommendation was made for community water systems that practice fluoridation of 0.7 mg/L, a reduction from the previous recommendation of 0.7–1.2 mg/L.[13]

[a]Department of Environmental Health Engineering, Mamasani Education Complex for Health, Shiraz University of Medical Sciences, Shiraz, Iran; [b]Health Promotion Research Centre and Department of Environmental Health Engineering, School of Public Health, Zahedan University of Medical Sciences, Zahedan, Iran; [c]Student Research Committee Zahedan University of Medical Sciences, School of Public Health, Department of Environmental Health Engineering, Zahedan, Iran; [d]Department of Environmental Health Engineering, School of Public Health, Tehran University of Medical Sciences, Tehran, Iran; [e]Center for Solid Waste Research, Institute for Environmental Research, Tehran University of Medical Sciences, Tehran, Iran; For correspondence: Associate Professor Amir Hossein Mahvi, Center for Solid Waste Research, Institute for Environmental Research, Tehran University of Medical Sciences, Tehran, Iran; E-mail: ahmahvi@yahoo.com

[Now published in full after the initial publication as an Epub ahead of print on July 11, 2021 at www.fluorideresearch.online/epub/files/131.pdf]

A number of drinking water defluoridation techniques have been developed.[14] Various traditional removal methods, such as precipitation, ion exchange, reverse osmosis, and oxidation, have been applied for the elimination of F^- from waste water but they have limitations such as being highly expensive and lacking the capacity to remove F^- at lower concentrations.[15-17] Also, secondary pollution may occur with the generation of toxic sludge and complicated procedures may be involved in the treatment.[18,19]

Biosorption has been suggested as a prospective technique for the reduction of toxic metal ions from contaminated effluent streams. This method has also been considered to be an efficient and cost-effective approach as it utilizes extensively accessible biomass from nature.[20] Among the numerous sorbent materials used for pollutant reduction, activated carbon, obtained from agricultural waste, has been identified as having excellent sorbent characteristics.[21] Activated carbons can be used in a broad and growing range of environmental, health, safety, and industrial applications as they have extremely high surface areas, varied porous structures, large adsorption capacities, and fast adsorption kinetics.[21] Many studies reveal that marine algae are one of the most important biosorbents with a high recovery for various pollutants, which results from the existence of distinct elemental groups in their cell membrane, like the hydroxyl, carboxyl, amino, and phosphate groups that play an essential role in the elimination of toxic contaminants from different industrial pollutants.[22]

In the present study, almond shells from almond waste were used as a F^- removal biosorbent due to the benefits of high efficiency, easy handling, cost-effectiveness, and their ready availability. The aim of the study was to examine the potential of ACAS in the removal of fluoride from aqueous solutions including assessing the effect on the fluoride removal efficiency of the parameters of contact time, initial F^- concentration, pH, and adsorbent dose.

MATERIAL AND METHODS

Adsorbent preparation: Almond shell was collected and washed several times with distilled water to remove adhered impurities from its surface. The biomass was dried at 105ºC for 2 hr. The dried biomass was milled and sieved to 10–100 m particle size. The dried mass was subjected to a carbonization process at 200ºC, then powdered well, and finally activated at a temperature of 500ºC for a period of 1 hr.

Adsorbent characteristics: The specific surface area of ASAC was determined by the BET-N_2 method based on nitrogen adsorption–desorption isotherms at 77K. Scanning electron microscopy (SEM) of the ASAC was carried out using a scanning electron microscope (EM3900M-KYKY). The FTIR spectra (Spectrum Two, Perkin Elmer) were recorded in the range of 400–4,000 cm^{-1} to find out the information regarding the bending vibrations and the stretching of the functional groups which are responsible for the adsorption process.

Sodium fluoride (NaF) was obtained from Merck. To prepare the primary solution of F (500 ppm), 0.1105 g NaF was dissolved into 500 mL distilled water and the next solutions are obtained by dilution.

[Now published if full after the initial publication as an Epub ahead of print on July 11, 2021 at www.fluorideresearch.online/epub/files/131.pdf]

Adsorption experiments: The examination of the removal characteristics of F^- was conducted in a controlled reaction mixture volume of 200 mL by using ACAS as a removal agent and varying the biosorption factors of contact time, adsorbent dose, pH, initial F^- strength, and biosorbent quantity. To prepare the stock solution of F^- (500 mg/L), 0.1105 g NaF was dissolved into 500 mL distilled water and the studied concentrations of the F^- solution were provided by diluting the stock solution. The pH of the solutions was adjusted to the desired value with 0.1M HCl and NaOH solutions. The adsorption experiments were carried out by the batch technique. For this, 100 mL of fluoride solution, in the concentration range of 2–20 mg/L, were transferred into an Erlenmeyer flask. Then, a certain amount of adsorbent (0.6 g/L) was added to the solution, and the mixture was agitated on a mechanical shaker at 150 rpm for 90 min. After reaching the equilibrium, the adsorbent was removed by vacuum filtration through 0.45 µm nitrocellulose membrane. The experiments were conducted with different process variables to estimate the sorption capability of ACAS, as a biosorbent, for F^-. The adsorbed quantity and the % removal of F^- through ACAS were determined by using Equations 1 and 2.[23]

$$\% \text{ Removal} = \frac{(C_0 - C_e)}{C_0} \times 100 \quad \text{.....Equation 1}$$

$$q_e = (C_0 - C_e) \times \frac{V}{M} \quad \text{.....Equation 2}$$

Where:

C_0 = the initial concentration of fluoride ion (F^-)
C_e = the final concentration of fluoride ion
q_e = the adsorption capacity for adsorbents (mg/L)
V = the fluoride ion solution volume (L)
M = the weight of the sorbent ACAS

The Langmuir model is described using the following equation (Equation 3).[24]

$$\frac{C_e}{q_e} = \frac{1}{Bq_e} + \frac{C_e}{q_{max}} \quad \text{.....Equation 3}$$

Where:

C_e = the equilibrium concentration of F^- (mg/L)
q_e = the amount of F^- adsorbed per unit weight of ACAS at equilibrium
B = the Langmuir constant representing the affinity of binding sites
q_{max} = the amount of F^- adsorbed on ACAS at maximum adsorption capacity (mg/g)

The Freundlich model, which is based on the surface heterogeneity of the adsorbent, is described using the following equation (Equation 4).[25-27]

[Now published in full after the initial publication as an Epub ahead of print on July 11, 2021 at www.fluorideresearch.online/epub/files/131.pdf]

$$\log q_e = \log K_F + \frac{1}{n} \log C_e \quad \text{..... Equation 4}$$

Where:

K_F = the Freundlich binding constant
C_e = the final concentration of fluoride ion
q_e = the adsorption capacity for adsorbents (mg/L)
1/n = the surface heterogeneity constant

The Temkin model is described using the following equation (Equation 5).[28]

$$q_e = \frac{Rt}{b} \ln K_T + \frac{RT}{b} \ln C_e, \quad \text{.....Equation 5}$$

Where:

K_T = the Temkin adsorption potential (1/g)
C_e = the final concentration of fluoride ion
q_e = the adsorption capacity for adsorbents (mg/L)
b = the Temkin constant

RESULTS

The SEM investigation was executed for the discovery of the surface characteristics and porosity of ACAS. The results obtained are shown in Figures 1A and 1B.

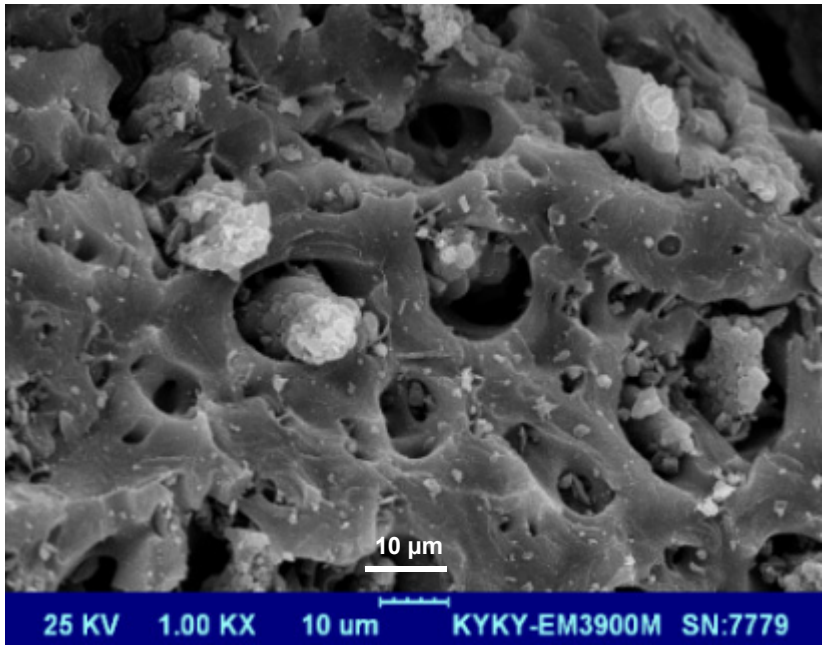

1A

Figure 1A. SEM analysis of ACAS before adsorption.

[Now published in full after the initial publication as an Epub ahead of print on July 11, 2021 at www.fluorideresearch.online/epub/files/131.pdf]

1B

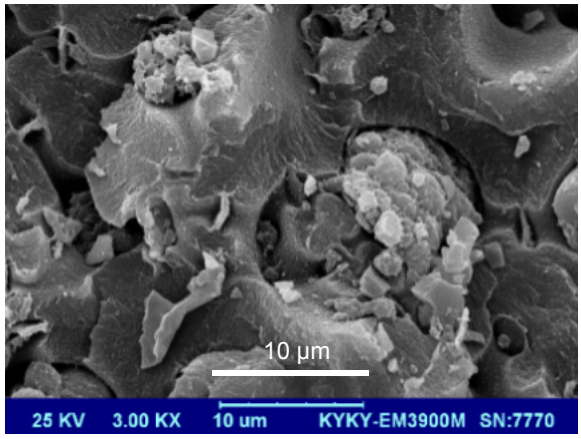

Figure 1B. SEM analysis of ACAS after adsorption.

The SEM micrograph exposed that the ACAS is extremely heterogeneous in nature and irregular along with a porous and rough surface morphology.

The total pore value, the average diameter, and the specific surface of ACAS were calculated and determined to be 0.241 cm^3/g, 1.73 nm, and 594.5 m^2/g, using BET theory, respectively.

To understand the interaction between the functional groups on the surface of ACAS and F^- were examined using FT-IR spectroscopy (Figure 2).

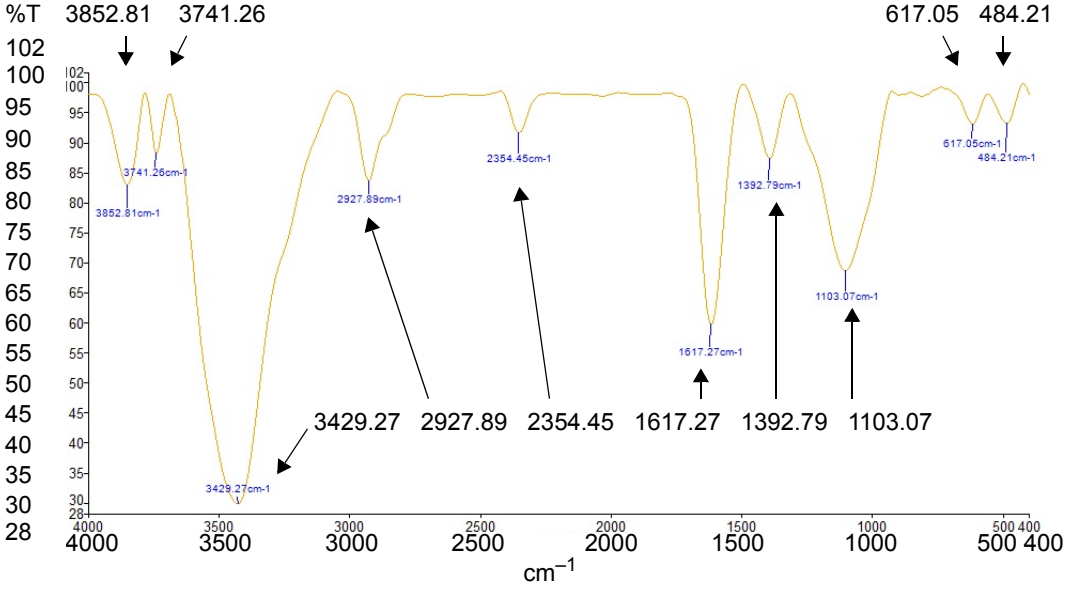

Figure 2. The FT-IR spectra of ASAC

The intense absorption peaks at around 3429 cm^{-1} correspond to the O–H stretching. The peaks at 2927 cm^{-1} are attributed to the symmetric and asymmetric C–H stretching vibration of aliphatic acids. The peak observed at 1617 cm^{-1} is the stretching vibration of the bond due to non-ionic carboxyl groups (–COOH, –

[Now published in full after the initial publication as an Epub ahead of print on July 11, 2021 at www.fluorideresearch.online/epub/files/131.pdf]

$COOCH_3$). The peaks at 1100 and 1400 cm^{-1} are due to asymmetric and symmetric stretching vibrations of C=O in ionic carboxylic groups (–COO-).

The effect of pH on fluoride removal is shown in Figure 3**.** With increasing pH, the F removal decreased.

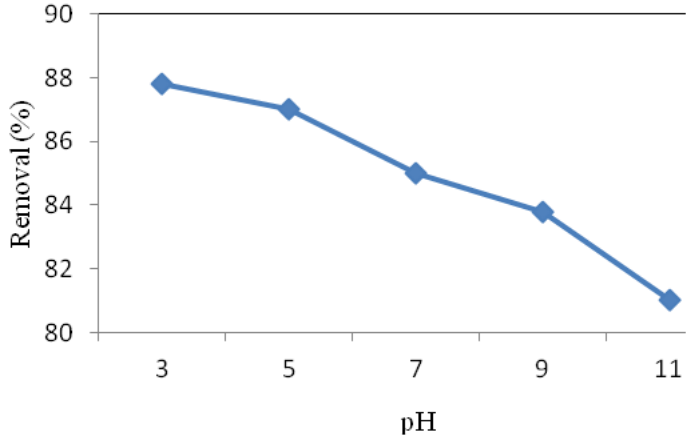

Figure 3. Effect of pH on fluoride ion (F^-) adsorption (adsorbent dose: 0.6 g/L, contact time: 90 min, and initial concentration of fluoride ion (C_0) = 20 mg/L).

The effect of contact time on the removal of F^- is shown in Figure 4. 81% F^- removal takes place in 60 min. The equilibrium was reached after 120 min.

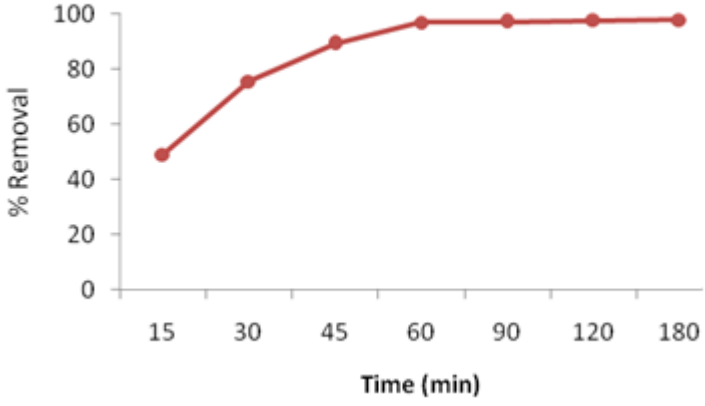

Figure 4. Effect of contact time on fluoride ion (F^-) adsorption (adsorbent dose: 1.0 g/L, pH = 3, and initial concentration of fluoride ion (C_0) = 20 mg/L).

Figure 5 shows the F^- removal efficiency of ACAS at various adsorbent doses. It is evident from Figure 5 that the F^- removal increased sharply with an increase in the dose adsorbent from 0.1 g to 1.0 g/L.

[Now published in full after the initial publication as an Epub ahead of print on July 11, 2021 at www.fluorideresearch.online/epub/files/131.pdf]

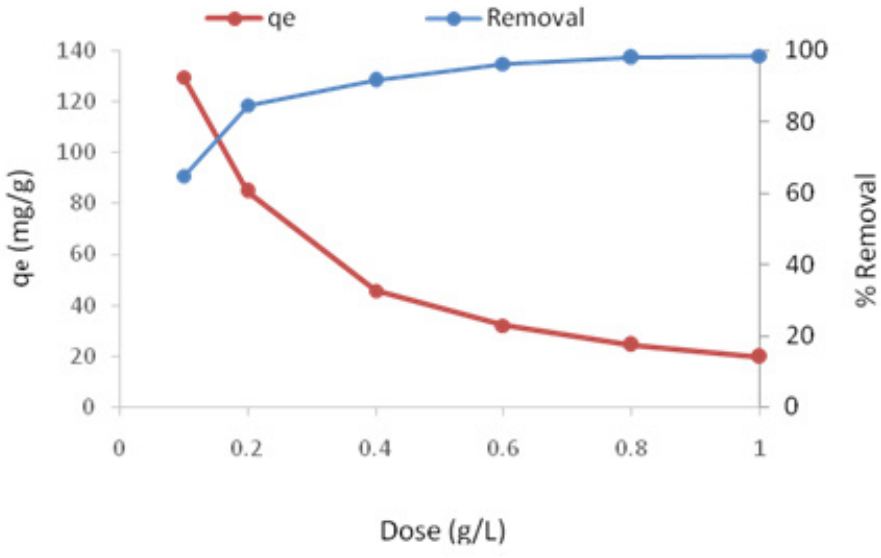

Figure 5. Effect of adsorbent dose on fluoride ion (F^-) adsorption (contact time: 90 min, initial concentration of fluoride ion (C_0) = 20 mg/L, and pH = 3).

The effect of F^- concentration on the adsorption of F^- on to ACAS was investigated in the concentration range of 2–20 mg/L and is shown in Figure 6. The equilibrium adsorption capacity increased with an increase in the F^- concentration.

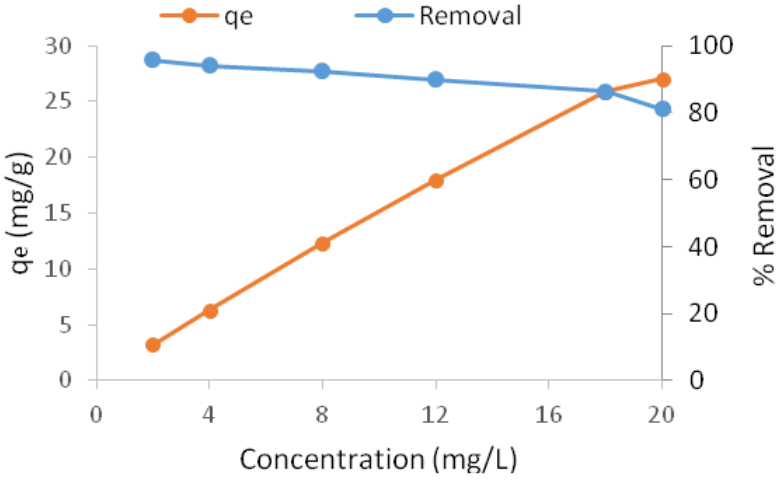

Figure 6. Effect of initial concentrations of fluoride ion (C_0) on fluoride ion (F^-) adsorption (contact time: 90 min, contact time: 90 min, and pH = 3).

Desorption isotherms: The adsorption of F^- on ACAS was studied using three isotherm models, the Langmuir, Freundlich, and Temkin models. The adsorption isotherm models help in describing the adsorption mechanism between the adsorbate

[Now published in full after the initial publication as an Epub ahead of print on July 11, 2021 at www.fluorideresearch.online/epub/files/131.pdf]

and the adsorbent. The Langmuir adsorption isotherm assumes that the adsorption takes place at specific homogeneous sites within the adsorbent and has found a successful application in many sorption processes of monolayer adsorption. In the aqueous phase processes, where the system does not fit as well, the three models of Langmuir, Freundlich, and Temkin were used to find a suitable mode for describing the process. The equilibrium data were was also evaluated for the isotherm models Table1.[29-31]

Table 1. Isotherms constants for the removal of fluoride ion (F^-) onto activated carbon developed from almond shell (ACAS)

Langmuir model				Freundlich model			Temkin model		
q_m	R_L	b	R^2	n	K_F	R^2	A_T	b	R^2
84.3	0.086	0. 212	0.998	2.71	0.495	0.843	4.31	184.6	0.974

The experimental data fitted well with the Langmuir model. The correlation factor, R^2, for the Langmuir model was found to be 0.998 while for the Freundlich and Temkin models R^2 was 0.843 and 0.974, respectively. The R^2 value for the Langmuir model was closer to unity than the values with the Freundlich and Temkin models.

Table 2 shows a comparison, from the literature, of the adsorption capacity (q_e) of different materials for adsorbing F^- from aqueous media under different experimental conditions.

Table 2. Comparison of the maximum uptake of fluoride ion (F^-) by various adsorbents

Adsorbent	q_e (mg/g)	Reference
Lemna minor	48.25	12
Chitosan	26.48	15
Leaf powder	38.71	13
Eggshell powder	65.9	19
Magnetic-chitosan particles	84.35	20
Hydrated cement	38.49	22
Nano-alumina	74.04	32
Cupricoxide nanoparticles	89.46	21

[Now published in full after the initial publication as an Epub ahead of print on July 11, 2021 at www.fluorideresearch.online/epub/files/131.pdf]

Kinetic studies: The pseudo-first order adsorption kinetics for the adsorption of the F^- on ACAS was studied using the following equation, which assumes that one adsorbate molecule is attached to one binding site of the adsorbent (Equation 6).[29]

$$\ln(q_e - q_t) = \ln q_e - k_1 t \quad \text{.....Equation 6}$$

Where:

q_e (mg/g) = the amount of adsorbed adsorbate at equilibrium
q_t (mg/g) = the amount of adsorbed adsorbate at time t
k_1 (min^{-1}) = the rate constant of pseudo-first order adsorption

A plot of Ln (q_e–q_t) versus t (the figure not shown) was used to determine the slope and intercept values. The adsorption kinetics can also be described using a pseudo-second order model, which assumes that one adsorbate molecule is adsorbed on to two active sites. The linear form of the pseudo-second order equation is given below (Equation 7).[30]

$$t/q_t = 1/k_2 q_e^2 + 1(t)/q_e \quad \text{.....Equation 7}$$

Where:

q_e (mg/g) = the amount of adsorbed adsorbate at equilibrium
q_t (mg/g) = the amount of adsorbed adsorbate at time t
k_2(min^{-1}) = the rate constant of pseudo-second order adsorption

The intra-particle diffusion kinetics, as depicted by Weber and Morris, can be described by the following equation for the assessment of mass transfer and the rate-determining steps (Equation 8).[31-32]

$$Qt = K_F t^{1/2} + C \quad \text{.....Equation 8}$$

Where:

K_F = the intra-particle rate constant
C = the boundary layer thickness

When the correlation coefficients were examined, the interaction between the surface of the ACAS and F^- seemed to fit the pseudo-second order kinetic model (Table 3). This was decided based on the R^2 and q_e values; for greater R^2 values (0.999) the q_e values (76.35 mg/g) are closer to those of the experimental results

[Now published in full after the initial publication as an Epub ahead of print on July 11, 2021 at www.fluorideresearch.online/epub/files/131.pdf]

(q_{exp}) (71.42 mg/g). Also, the adsorption capacity values obtained from the pseudo-second order kinetic model are in good agreement with the experimental results.

Table 3. Kinetic parameters for the adsorption of the fluoride ion (F^-) on to activated carbon developed from almond shell (ACAS)

Adsorption kinetics model								
Pseudo-first order			Pseudo-second order			Intra-particle diffusion		
K_1	q_e (mg/g)	R^2	K_2	q_e (mg/g)	R^2	K_F	I	R^2
0.0147	21.75	0.842	0.0048	76.35	0.999	0.278	2.761	0.935

According to the graphs drawn, the intra-particle diffusion (IPD) model showed no linearity and the R^2 values obtained were smaller than 1 (Figure 7). Therefore, it was found that the adsorption in our system was not at the intra-particle level (Table 2).

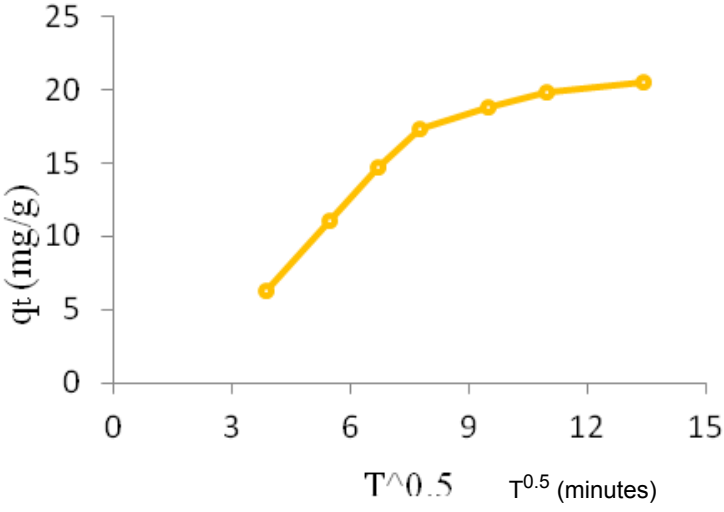

Figure 7. Intra-particle diffusion kinetics toward the elimination of the fluoride ion (F^-).

DISCUSSION

According to Figure 3, with increasing pH, the F^- removal decreased. This was probably due to an inappropriate surface charge and to competition for the adsorption sites because of the presence of excess anion in the alkaline conditions. However, there were no significant differences in F^- removal. This finding is in agreement with the literature.[26,27] About 81% of F^- removal takes place in 60 min. The equilibrium was reached after 120 min (Figure 4). The fluoride removal process was incremental

[Now published in full after the initial publication as an Epub ahead of print on July 11, 2021 at www.fluorideresearch.online/epub/files/131.pdf]

from 60 minutes to 120 minutes. Due to the small difference in the removal rate from 60 to 120 minutes, the contact time of 90 minutes was selected for the tests.

As shown in Figure 5, the F^- removal increased sharply with an increase in the dose of adsorbent from 0.1 g/L to 1 g/L. The change in the rate of adsorption might be due to fact that initially all the adsorbent sites are vacant and the solute concentration gradient is very high.[33,34] Later, the lower adsorption rate is due to a decrease in number of vacant sites on the adsorbent and a decrease in the F^- concentrations.[26,27] The decreased adsorption rate, particularly, toward the end of the experiments, indicates a possible monolayer formation of F^-on the adsorbent surface. This may be attributed to a lack of the available active sites required for further uptake after attaining the equilibrium.[35] This may be due to the availability of more ACAS sites as well as a greater availability of specific surfaces on the adsorbents.[36] However, no significant changes in removal efficiency were observed beyond the ACAS dose of 0.6 g/L. Due to the conglomeration of ACAS particles, there is no increase in the effective surface area of ACAS with higher doses of ACAS. So, 0.6 g/L was considered to be the optimal dose for ACAS loading.

The results of the study showed that the equilibrium adsorption capacity increased with an increase in the F^- concentration. Further increases in the F^- concentration did not result in any significant changes in the removal efficiency (Figure 6). This is due to the fact that with increased F^- concentrations the driving force for transfer also increases.[37] At low concentrations there will be unoccupied active sites on the adsorbent surface.[38]

The Freundlich model is used to explain physical adsorptions taking place on the surface of heterogeneous adsorbents. It is assumed that each functional region on the surface of the adsorbent has a different adsorption potential. According to our findings, the regions where the adsorption events occur on the surface of the ACAS have the same potential making the system fit better with the Langmuir model. Since it fits the Langmuir model, the equilibrium was proven to be reached, at a constant temperature, between the concentration of F^- in the environment and the concentration of the F^- that was adsorbed as a single layer on the ACAS which was assumed to be homogeneous. Due to the better suitability of the Langmuir model, the saturation of the adsorbent surface was also proven. Moreover, with the finding that the material had a homogenous structure, the confirmation of the characterization was also established.[30-32]

The rate control mechanism depends on 3 possible steps during the adsorption process. The first one is the mass transfer to the outer surface at the early stages of the adsorption or film diffusion. This is followed by the second step of the reaction or constant rate step. The third and last step, involves the diffusion towards the inner parts of the pores where the adsorption amount is significantly decreased. These rate control mechanisms are explained with the pseudo-first order and the pseudo-second order kinetic models.[39]

If the adsorption rate determining step is based on the diffusion of the F^- to the surface of the adsorbent, the system fits the pseudo-first order model. If the adsorption rate determining step is based on the interaction between the F^- and the adsorbent, the system fits the pseudo-second order model. The first case is called a

[Now published in full after the initial publication as an Epub ahead of print on July 11, 2021 at www.fluorideresearch.online/epub/files/131.pdf]

diffusion-controlled process and the second one is referred to as chemisorption. The treatment and exposure times are important to understand the steps affecting adsorption rates.[38,39] The mechanisms controlling the adsorption process are mass transfer and chemical reactions. In the determination of these mechanisms, the pseudo-first and second order models were applied to the experimental data. When the kinetic data were analyzed it was found that the adsorption of F^- on to ACAS was chemisorption without any diffusion restriction.[40]

CONCLUSIONS

We report here an effective strategy for the removal of F^- using ACAS complexes. The ACAS was found to exhibit a F^- removal efficiency of 99.2%. The adsorption of F^- on ACAS was found to follow the Langmuir adsorption isotherm model and the pseudo-second order kinetics. The production of ACAS, within the scope of this study, is safe and cost-efficient, which makes this green adsorbent a good candidate for the removal of F^- from water resources. This study represents the first F^- adsorption study based on AC obtained from almond shell.

ACKNOWLEDGEMENT

The authors are grateful to the Zahedan University of Medical Sciences, Zahedan, Iran for the financial support to conduct this work with code 7842.

REFERENCES

1 Rahmani A, Rahmani K, Dobaradaran S, Mahvi AH, Mohamadjani R, Rahmani H. Child dental caries in relation to fluoride and some inorganic constituents in drinking water in Arsanjan, Iran. Fluoride 2010;43(3):179-86,.

2 Dobaradaran S, Fazelinia F, Mahvi AH, Hosseini SS. Particulate airborne fluoride from an aluminium production plant in Arak, Iran. Fluoride 2009;42(3):228-32.

3 Rahmani A, Rahmani K, Mahvi AH, Usefie M. Drinking water fluoride and child dental caries in Noorabademamasani, Iran. Fluoride 2010;43(3):187-93.

4 Dobaradaran S, Mahvi AH, Dehdashti S, Dobaradaran S, Shoara R. Correlation Of fluoride with some inorganic constituents in groundwater of Dashtestan, Iran. Fluoride 2009;42(1):50-3.

5 Biglari H, Chavoshani A, Javan N, Mahvi AH. Geochemical study of groundwater conditions with special emphasis on fluoride concentration, Iran. Desalination and Water Treatment 2016; 57(47):22392-7.

6 Dobaradaran S, Mahvi AH, Dehdashti S, Abadi DRV. Drinking water fluoride and child dental caries in Dashtestan, Iran. Fluoride2008; 41(3):220-6.

7 Mahvi AH., Zazoli MA, Younesian M, Nicpour B, Babapour A. Survey of fluoride concentration in drinking water sources and prevalence of DMFT in the 12 years old students in Behshar City. Journal of Medical Sciences 2006;6(4):658-61.

8 Yousefi M, Ghoochani M, Mahvi AH. Health risk assessment to fluoride in drinking water of rural residents living in the Poldasht city, Northwest of Iran. Ecotoxicology and Environmental Safety 2018;148:426-30.

9 Mohammadi AA, Yousefi M, Yaseri M, Jalilzadeh M, Mahvi AH. Skeletal fluorosis in relation to drinking water in rural areas of West Azerbaijan, Iran. Scientific Reports 2017;7(1):44-51. Article number 17300.

10 Aghaei M, Derakhshani R, Raoof M, Dehghani M, Mahvi AH. Effect of fluoride in drinking water on birth height and weight: an ecological study in Kerman Province, Zarand County, Iran. Fluoride 2015;48(2):160-8.

[Now published in full after the initial publication as an Epub ahead of print on July 11, 2021 at www.fluorideresearch.online/epub/files/131.pdf]

11 Karimzade S, Aghaei M, Mahvi AH. Investigation of intelligence quotient in 9–12-year-old children exposed to high and low drinking water fluoride in west Azerbaijan province, Iran. Fluoride 2014;47(1):9-14.

12 Zazouli MA, Balarak D, Karimnezhad F, Khosravi F. Removal of fluoride from aqueous solution by using of adsorption onto modified *Lemna minor*: adsorption isotherm and kinetics study. Journal of Mazandaran University Medical Sciences 2014;23(109):208-17.

13 Spittle B. A step in the right direction [editorial]. Fluoride 2015;48(2):91-2.

14 WHO. Chemical fact sheets: fluoride. 3rd ed. Guidelines for drinking water quality (electronic resource): Incorporating the first addendum. Recommendations 2006. vol 1. Geneva: WHO; 2006. pp. 375-7.

15 Bazrafshan E, Ownagh KA, Mahvi AH. Application of electrocoagulation process using iron and aluminum electrodes for fluoride removal from aqueous environment. E-Journal of Chemistry 2012;9(4):2297-308.

16 Akbari H, Jorfi S, Mahvi AH, Yousefi M, Balarak D. Adsorption of fluoride on chitosan in aqueous solutions: determination of adsorption kinetics. Fluoride 2018;51(4):319-27.

17 Somak C, Sirshendu D. Adsorptive removal of fluoride by activated alumina doped cellulose acetate phthalate (CAP) mixed matrix membrane. Separation and Purification Technology 2014;125:223-38.

18 Bharali R, Bhattacharyya K, Krishna G. Biosorption of fluoride on Neem (*Azadirachta indica*) leaf powder. Journal of Environmental Chemical Engineering 2015;3(2):662-9.

19 Zhen J, Yong J, Kai-Sheng Z. Effective removal of fluoride by porous MgO nanoplates and its adsorption mechanism. Journal of Alloys and Compounds 2016;675:292-300.

20 Bhaumik R, Mondal NK, Das B, Roy P, Pal KC, Datta JK. Eggshell powder as an adsorbent for removal of fluoride from aqueous solution: Equilibrium, kinetic and thermodynamic studies. J Chem 2012;9:1457-80.

21 Ma W, Ya FQ, Han M, Wang RJ. Characteristics of equilibrium, kinetics studies for adsorption of fluoride on magnetic-chitosan particle. J Hazard Mater 2007;143:296-302.

22 Bazrafshan E, Balarak D, Panahi AH, Kamani H, Mahvi AH. Fluoride removal from aqueous solutions by cupricoxide nanoparticles. Fluoride 2016;49(3 Pt 1);233-44.

23 Kagne S, Jagtap S, Dhawade Kamble SP, Devotta S, Rayalu SS. Hydrated cement: a promising adsorbent for the removal of fluoride from aqueous solution, J Hazard Mater 2008; 154:88-95.

24 Kumar E, Bhatnagar A, Kumar U, Sillanpaa M. Defluoridation from aqueous solutions by nano-alumina: Characterization and sorption studies. J Hazard Mater 2011;186:1042-9.

25 Tor A. Removal of fluoride from an aqueous solution by using montmorillonite. Desalination 2006;201:267-76.

26 Mourabet M, El-Boujaady H, El-Rhilassi A, Ramdane H, Bennani-Ziatni M. Defluoridation of water using Brushite: equilibrium, kinetic and thermodynamic studies. Desalination 2011;278: 1-9.

27 Sun Y, Fang Q, Dong J, Cheng X, Xu J. Removal of fluoride from drinking water by natural stilbite zeolite modified with Fe(III). Desalination 2011;277: 121-7.

28 Meenakshi D, Maheshwari RC. Fluoride in drinking water and its removal. J Hazard Mater 2006;137(1):456-63.

29 Zazouli MA, Mahvi AH, Mahdavi Y, Balarak D. Isothermic and kinetic modeling of fluoride removal from water by means of the natural biosorbents sorghum and canola. Fluoride 2015; 48(1):37-44.

30 Chen N, Zhang Z, Feng C, Sugiura N, Li M, Chen R. Fluoride removal from water by granular ceramic adsorption. Adv Colloid Interface Sci 2010;348:579-84.
31 Srivastav AL, Singh PK, Srivastava V, Sharma YC. Application of a new adsorbent for fluoride removal from aqueous solutions. J Hazard Mater 2013;263:342-52.
32 Zhang Z, Niu Y, Chen H, Yang Z, Bai L, Xue Z, Yang H. Feasible one-pot sequential synthesis of aminopyridine functionalized magnetic Fe_3O_4 hybrids for robust capture of aqueous Hg(II) and Ag(I). ACS Sustainable Chem Eng 2019;7(7):7324-37.
33 Boldaji MR, Mahvi AH, Dobaradaran S, Hosseini SS. Evaluating the effectiveness of a hybrid sorbent resin in removing fluoride from water. International Journal of Environmental Science and Technology 2009;6(4):629-32.
34 Haghighat GA, Dehghani MH, Nasseri S, Mahvi AH, Rastkari N. Comparison of carbon nonotubes and activated alumina efficiencies in fluoride removal from drinking water. Indian Journal of Science and Technology 2012;5(23): 2432-5.
35 Zazouli MA, Mahvi AH, Dobaradaran S, Barafrashtehpour M, Mahdavi Y, Balarak D. Adsorption of fluoride from aqueous solution by modified *Azolla filiculoides*. Fluoride 2014;47(4):349-58.
36 Zhou Y, Luan L, Tang B, Niu Y, Qu R, Liu Y, Xu W. Fabrication of Schiff base decorated PAMAM dendrimer/magnetic Fe_3O_4 for selective removal of aqueous Hg(II). Chemical Engineering Journal 2020;398:125651.
37 Balarak D, Mostafapour FK, Bazrafshan E, Mahvi AH. The equilibrium, kinetic, and thermodynamic parameters of the adsorption of the fluoride ion on to synthetic nano sodalite zeolite. Fluoride 2017;50(2):223-34.
38 Li YH, Wang S, Cao A, Zhao D, Zhang X, Xu C, Luan Z. Adsorption of fluoride from water by amorphous alumina supported on carbon nanotubes. Chem Phys Lett 2010;350:412-6.
39 Yu XL, Tong SR, Ge MF, Zuo JC. Removal of fluoride from drinking water by cellulose-hydroxyapatite nanocomposites. Carbohyd Polym 2013;92:269-75.
40 Song X, Niu Y, Qiu Z, Zhang Z, Zhou Y, Zhao J, Chen H Adsorption of Hg(II) and Ag(I) from fuel ethanol by silica gel supported sulfur-containing PAMAM dendrimers: kinetics, equilibrium and thermodynamics. Fuel 2017;206:80-8.